UC Davis

UC Davis Previously Published Works

Title

Painting and dissecting Epidermolysis Bullosa Simplex-associated keratin aggregates

Permalink

https://escholarship.org/uc/item/2fn5v54x

Authors

Rietscher, Katrin
Homberg, Melanie
Kovalenko, Ilya
et al.

Publication Date

2023-08-01

DOI

10.1016/j.jdermsci.2023.08.007

Peer reviewed

Painting and dissecting Epidermolysis Bullosa Simplex-associated keratin aggregates

[1]Katrin Rietscher*, [1]Melanie Homberg, [2,3,4,5]Ilya Kovalenko, [2,3,4]Jonathan Z. Sexton, [6,7]Robert H. Rice, [8]Cristina Has, [9]M. Bishr Omary and [1]Thomas M. Magin

[1]Institute of Biology, Professorship of Cell and Developmental Biology, University of Leipzig, 04103 Leipzig, Germany

[2]Department of Medicinal Chemistry, College of Pharmacy, University of Michigan, Ann Arbor, MI, 48109, USA

[3]Department of Internal Medicine, Gastroenterology and Hepatology, Michigan Medicine at the University of Michigan, Ann Arbor, MI, 48109, USA

[4]U-M Center for Drug Repurposing, University of Michigan, Ann Arbor, MI, 48109, USA

[5]Insilico Medicine HK Limited, Unit 307A, Core Building 1, No. 1 Science Park East Avenue, Science Park, Hong Kong

[6]Department of Environmental Toxicology, University of California, Davis, California, 95616, USA

[7]Forensic Science Program, University of California, Davis, California, 95616, USA

[8]Department of Dermatology, Medical Center, University of Freiburg, Freiburg, Germany

[9]Center for Advanced Biotechnology and Medicine, and Robert Wood Johnson Medical School, Rutgers University, Piscataway, New Jersey, USA

*Corresponding Author:

Katrin Rietscher, Institute of Biology, Professorship of Cell and Developmental Biology, University of Leipzig, Philipp-Rosenthal-Str. 55, D-04103 Leipzig, Germany, phone 0049 (0) 341 97 39587, katrin.rietscher@uni-leipzig.de

Conflict of interest:

The authors have no conflict of interest to declare.

Text word count: 1000, **Number of references**: 10, **Figures**: 2

LETTER TO THE EDITOR

Protein aggregates are common denominators of many neuromuscular pathologies such as Huntington´s disease, Alzheimer´s disease and familial amyotrophic lateral sclerosis [1]. The distinct morphology, localization and composition of corresponding aggregates raises the question, whether they display common and distinctive features that can be exploited for diagnosis or therapy. Some protein aggregates, such as inclusion bodies and aggresomes, are believed to be protective by sequestering misfolded proteins for degradation. Epidermolysis Bullosa Simplex (EBS), an inherited blistering skin disease, is also characterized by the formation of electron-dense, cytoplasmic aggregates in tissues and patient-derived keratinocytes [2, 3]. Such aggregates are characteristic for the most severe form of EBS (OMIM 131760) and are immuno-reactive for antibodies to keratins 5 and 14 (K5, K14). These keratins form the major intermediate filament cytoskeleton of the basal epidermis and provide essential contact to the underlying dermis via interactions with hemidesmosomes along the basement membrane. The primary causes of EBS are sequence variations in either of the genes encoding K5 or K14. The observation that EBS-associated mutant keratins form extensive filaments but rarely aggregates *in vitro* [4] suggests that the contribution of additional factors to keratin aggregation, such as posttranslational modifications and/or associated proteins. Recently, we showed that EBS-associated K5/K14 sequence variations alter phosphorylation of keratins [5] and of associated proteins, such as desmoplakin, thereby enhancing disease severity. Conversely, treatment with the multi-kinase inhibitor PKC412 reduced keratin aggregation and promoted restoration of an extended epidermal keratin filament network [6]. During these studies, we discovered that the dye CellMask red stain (CMR), marketed for labeling the cytoplasm and nucleus of cells, specifically stained K5/K14 keratin

aggregates in two different patient-derived immortalized EBS cell lines, K14.R125C and K14.R125G (Fig. 1a and S1a/b, untreated).

To investigate the specificity of CMR, normal human keratinocytes (NHK) were stained and showed no CMR-stained dots (Fig. 1b). Upon PKC412 and vehicle treatment of K14.R125C keratinocytes, cells were co-stained for CMR and anti-K14. This revealed markedly fewer and smaller CMR-positive aggregates in PKC412-treated as compared with DMSO-treated keratinocytes (Fig. 1b-1b′). Line scans of K14 and CMR fluorescence intensities across keratin aggregates from DMSO-treated K14.R125C keratinocytes showed the highest fluorescence intensity of CMR within keratin aggregates. Upon PKC412 treatment, the fluorescence intensity signals of K14 and CMR in the remaining keratin aggregates were weaker and smaller (Fig. 1b′′). Unlike electron microscopy images, showing filled, electron-dense clumps of keratins [3], fluorescence microscopy typically revealed K5- or K14-positive ring-like structures, indicating that in some cases keratin antibodies failed to penetrate the center of aggregates (Fig. 1b′, [7]). In contrast, CMR stains the aggregates homogeneously, with the strongest signal being in the middle of the keratin aggregates. To examine whether the CMR-positive keratin aggregates contained hyperphosphorylated keratins, staining with a phospho-site specific antibody recognizing phospho-T150 of the conserved LLS/TPL sequence motif in K5 [8] was performed [5]. This confirmed the presence of phosphorylated K5 at T150 predominantly in K5-positive aggregates of K14.R125C keratinocytes, whereas limited if any P-K5-positive signals were detectable in NHK (Fig. S1c).

Consistently, PKC412 treatment also reduced the keratin aggregates in K14.R125G keratinocytes, which was also readily visible by a reduction of the CMR signal (Fig. S1b), suggesting similar labelling of K14.R125C and K14.R125G protein aggregates by CMR. Thus, CMR staining of epidermal keratin aggregates represents an innovative and highly

sensitive tool for automated acquisition and analysis in image-based high-content screening assays. Whether it is applicable for easy diagnosis of EBS on tissue sections remains to be studied.

As a first step to identify CMR targets, we exploited the unique setting of keratin-deficient murine keratinocytes (KtyI^{-/-}) to investigate the composition of EBS-associated keratin aggregates. In these cells, stable expression of the EBS-associated mouse K14.R131P variant (equivalent to human K14.R125P) together with wildtype (WT) K5 resulted in formation of aggregates but no filaments (Fig. 2a). WT K14 and K5, along with KtyI^{-/-} served as controls. As predicted, CMR stained K14-positive aggregates in K14.R131P transfectants, whereas in WT cells a diffuse cytoplasmic staining pattern was observed (Fig. 2a). The above setting enabled enrichment of highly insoluble, K14.R131P/K5 aggregates in the absence of filaments in comparison to WT filaments by detergent/high ionic strength buffers. To ascertain that aggregated keratins were indeed insoluble, as reported for keratin filaments [9], mutant cells containing K14.R131P-positive aggregates and WT K14 controls grown on coverslips were extracted with Triton X-100. Following extraction of soluble proteins, K14-positive aggregates in the former and K14-positive filaments were immunostained after Triton X-100 extraction (Fig. 2b, KtyI^{-/-} K14; KtyI^{-/-} K14.R131P). To compare keratin-associated proteins enriched in aggregates to those in WT cells containing filaments, cytoskeletal fractionation was performed. Immunoblotting detected high and low amounts of K14 in insoluble and soluble fractions of K14.R131P and WT cells and no K14 in KtyI^{-/-} cells, respectively (Fig. 2c). Next, a proteome analysis of insoluble fractions from K14.R131P and WT cells was performed (Suppl. table 2). The analysis of proteins enriched in the insoluble fractions of K14.R131P and control keratinocytes is shown in Fig. 2d. Keratin 5 (Krt5), keratin 7 (Krt7), plectin (Plec) and non-muscle myosin heavy chain IIA (Myh9) were enriched to a greater extent

in the insoluble fractions of mutant compared to WT keratin 14 cells (Fig. 2d). Keratin 14 (Krt14), keratin 6a (Krt6a), the desmosomal proteins plakophilin 1 (Pkp1), desmoplakin (Dsp) and plakoglobin (Jup), a component of desmosomes and adherens junctions were also enriched in K14 aggregates, but to a lesser extent compared to their insoluble counterparts in WT cells. Notably, Myh9 was recently described as a protein that associated with keratins in a myosin dephosphorylation-dependent manner [10]. Whether these proteins, possibly in an altered conformation or upon posttranslational modification, are involved in keratin aggregation or CMR staining, requires future investigation. We cannot exclude the possibility that constituents of aggregates, which are extracted by the buffers used in this study, are involved in CMR staining. Our discovery of CMR as a stain for epidermal keratin aggregates invites the comparative analysis of additional protein aggregates, the identification of which might be useful for a deeper understanding of mechanisms involved in protein aggregation.
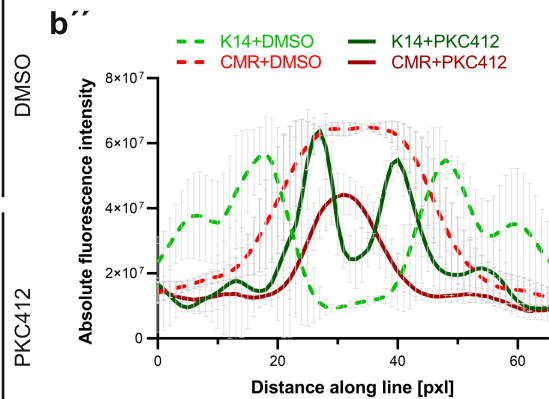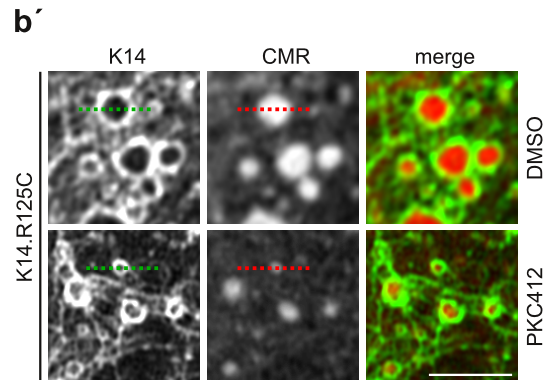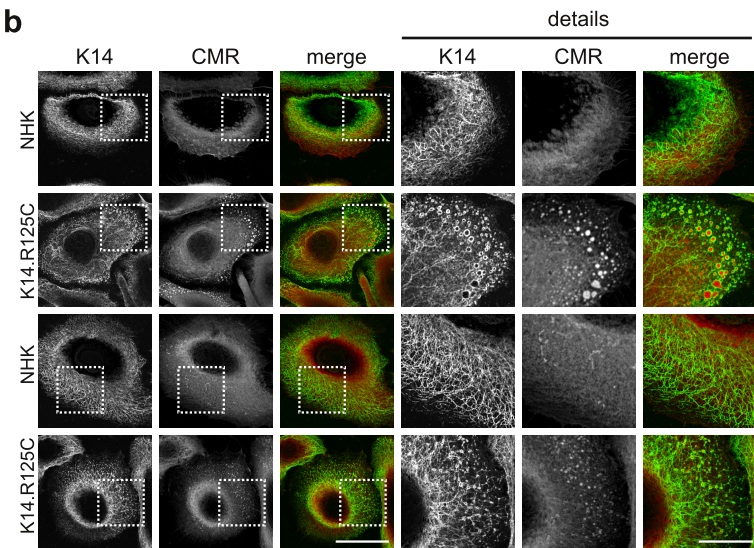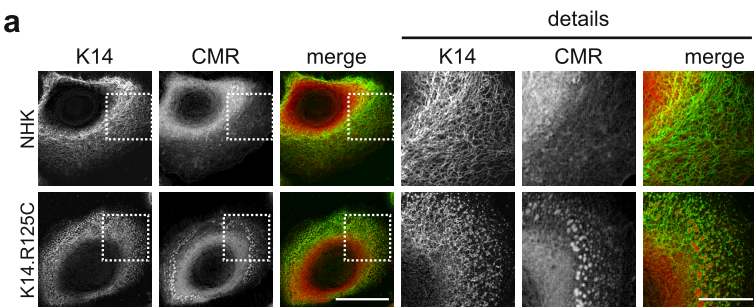
FIGURE LEGENDS

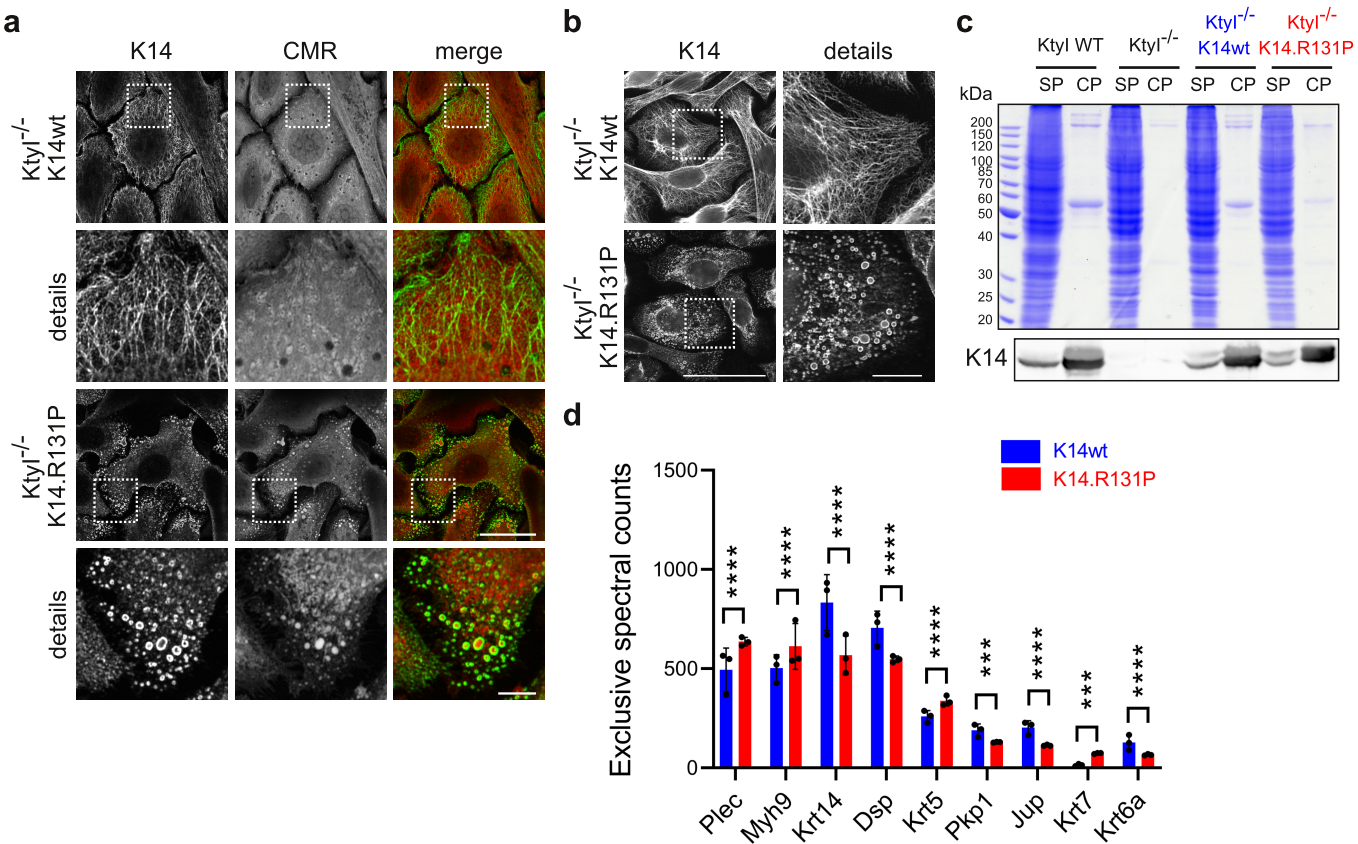**Figure 1: CMR dye stains EBS-associated keratin aggregates**

(a) Immortalized patient-derived K14.R125C and normal human keratinocytes (NHK) were analyzed by immunofluorescence microscopy showing K14 and CellMask Red (CMR) dye staining. Depicted are confocal images of single optical sections. The enlargements highlight the labeling of keratin aggregates by CMR. Scale bar: 25µm, details: 10µm. **(b)** NHK and EBS K14.R125C keratinocytes were treated with 0.8µM PKC412 or DMSO for 24h, respectively, and immunostained for K14 and CMR. Depicted are confocal images of single optical sections. Scale bar: 25µm, details: 10µm. **(b′)** To highlight the labeling of keratin aggregates in K14.R125C cells by CMR, detailed images of DMSO- and PKC412-treated keratinocytes from (b) are shown. The green and red dotted lines show the principle of line scan analysis of K14 (green) and CMR (red) fluorescence intensities across keratin aggregates. Scale bar: 2.5µm. **(b′′)** Representative line scans of K14 and CMR fluorescence intensities across keratin aggregates from K14.R125C keratinocytes treated with PKC412 (aligned) or DMSO (dashed), respectively (mean±SD, *n*=3).

Figure 2: Analysis of the insoluble fractions from K14wt and K14.R131P keratinocytes

(a) KtyI$^{-/-}$ K14wt and K14.R131P keratinocytes were analyzed by immunofluorescence microscopy showing K14 and CellMask Red (CMR) dye. Depicted are confocal images of single optical sections. The enlargements highlight the labeling of keratin aggregates in K14.R131P keratinocytes by CMR. Scale bar: 25µm, details: 5µm. **(b)** Immunofluorescence after extraction of soluble proteins with Triton X-100 shows that K14 positive keratin filaments (top panels, KtyI$^{-/-}$ K14wt) as well as K14 positive

aggregates (lower panels, KtyI$^{-/-}$ K14.R131P) are insoluble. Scale bar: 50μm, details: 10μm. **(c)** Cytoskeletal fractionation reveals presence of K14 in the soluble (S) and insoluble cytoskeletal/pellet (P) fraction as shown by the Coomassie-stained SDS gel (upper panel) and corresponding immunoblot for K14 (lower panel). WT and KtyI$^{-/-}$ keratinocytes are shown as control. **(d)** Mass spectrometry analysis of insoluble fractions from KtyI$^{-/-}$ K14wt (blue) and K14.R131P (red) keratinocytes after cytoskeletal fractionation showed by exclusive spectral counts. Note that the insoluble fractions of K14.R131P cells contain more plectin (Plec), NMHC-IIA (Myh9), K5 (Krt5) and K7 (Krt7) and less K14 (Krt14), desmoplakin (Dsp), plakophilin 1 (Pkp1), plakoglobin (Jup) and K6a (Krt6a) compared to the insoluble fractions of K14wt keratinocytes (mean±SD, n=3, 2way-ANOVA, Sidak′s multiple comparisons test, ***P<0.0005, ****P<0.0001).

a

| | K14 | CMR | merge | details K14 | CMR | merge |

NHK

K14.R125C

b

| | K14 | CMR | merge | details K14 | CMR | merge |

DMSO

NHK

K14.R125C

PKC412

NHK

K14.R125C

b´

| | K14 | CMR | merge |

K14.R125C

DMSO

PKC412

b´´

Legend:
- K14+DMSO (green dashed)
- CMR+DMSO (red dashed)
- K14+PKC412 (green solid)
- CMR+PKC412 (dark red solid)

Y-axis: Absolute fluorescence intensity (8×10^7, 6×10^7, 4×10^7, 2×10^7, 0)

X-axis: Distance along line [pxl] (0, 20, 40, 60)

a

K14 | CMR | merge

Ktyl⁻/⁻ K14wt

details

Ktyl⁻/⁻ K14.R131P

details

b

K14 | details

Ktyl⁻/⁻ K14wt

Ktyl⁻/⁻ K14.R131P

c

Ktyl WT | Ktyl⁻/⁻ | Ktyl⁻/⁻ K14wt | Ktyl⁻/⁻ K14.R131P

SP CP | SP CP | SP CP | SP CP

kDa
200
150
100
85
70
60
50
40
30
25
20

K14

d

K14wt
K14.R131P

Exclusive spectral counts

Plec Myh9 Krt14 Dsp Krt5 Pkp1 Jup Krt7 Krt6a

**** **** **** **** **** *** **** *** ****

REFERENCES

[1] J.A.J. Housmans, G. Wu, J. Schymkowitz, F. Rousseau, A guide to studying protein aggregation, FEBS J 290(3) (2023) 554-583.

[2] I. Anton-Lamprecht, Ultrastructural identification of basic abnormalities as clues to genetic disorders of the epidermis, The Journal of Investigative Dermatology 103(5 Suppl) (1994) 6S-12S.

[3] A. Ishida-Yamamoto, J.A. McGrath, S.J. Chapman, I.M. Leigh, E.B. Lane, R.A. Eady, Epidermolysis bullosa simplex (Dowling-Meara type) is a genetic disease characterized by an abnormal keratin-filament network involving keratins K5 and K14, The Journal of Investigative Dermatology 97(6) (1991) 959-68.

[4] H. Herrmann, T. Wedig, R.M. Porter, E.B. Lane, U. Aebi, Characterization of early assembly intermediates of recombinant human keratins, Journal of Structural Biology 137(1-2) (2002) 82-96.

[5] M. Sawant, N. Schwarz, R. Windoffer, T.M. Magin, J. Krieger, N. Mucke, et al., Threonine 150 Phosphorylation of Keratin 5 Is Linked to Epidermolysis Bullosa Simplex and Regulates Filament Assembly and Cell Viability, The Journal of Investigative Dermatology 138(3) (2018) 627-636.

[6] K. Rietscher, H.G. Jahnke, M. Rübsam, E.W. Lin, C. Has, M.B. Omary, et al., Kinase Inhibition by PKC412 Prevents Epithelial Sheet Damage in Autosomal Dominant Epidermolysis Bullosa Simplex through Keratin and Cell Contact Stabilization, The Journal of Investigative Dermatology 142(12) (2022) 3282-3293.

[7] D. Russell, P.D. Andrews, J. James, E.B. Lane, Mechanical stress induces profound remodelling of keratin filaments and cell junctions in epidermolysis bullosa simplex keratinocytes, Journal of Cell Science 117(Pt 22) (2004) 5233-43.

[8] D.M. Toivola, Q. Zhou, L.S. English, M.B. Omary, Type II keratins are phosphorylated on a unique motif during stress and mitosis in tissues and cultured cells, Molecular Biology of the Cell 13(6) (2002) 1857-70.

[9] M.B. Omary, "IF-pathies": a broad spectrum of intermediate filament-associated diseases, The Journal of Clinical Investigation 119(7) (2009) 1756-62.

[10] R. Kwan, L. Chen, K. Looi, G.Z. Tao, S.V. Weerasinghe, N.T. Snider, et al., PKC412 normalizes mutation-related keratin filament disruption and hepatic injury in mice by promoting keratin-myosin binding, Hepatology 62(6) (2015) 1858-69.

SUPPLEMENTARY MATERIAL FOR

Painting and dissecting Epidermolysis Bullosa Simplex-associated keratin aggregates

Katrin Rietscher*, Melanie Homberg, Ilya Kovalenko, Jonathan Z. Sexton, Robert H. Rice, Cristina Has, M. Bishr Omary and Thomas M. Magin

#To whom correspondence should be addressed.

E-Mail: katrin.rietscher@uni-leipzig.de

This PDF file includes:

Supplementary materials and methods

Supplementary figure legend

Supplementary table

Supplementary references

Supplementary figure

SUPPLEMENTARY MATERIALS AND METHODS

Cell lines and inhibitor treatment

Immortalized human control (NHK, normal human keratinocytes) and EBS keratinocytes (K14.R125C and K14.R125G) were established and cultured as described previously (Has *et al.*, 2018; He *et al.*, 2016). For PKC412 treatment, NHK, K14.R125C or K14.R125G keratinocytes were seeded in medium without treatment. Next day, cells were washed twice with PBS, the medium was changed to fresh medium supplemented with 0.8 µM PKC412 (Biomol) or vehicle-control (DMSO) and incubated for 24h. Mouse keratinocytes (KtyI WT, KtyI$^{-/-}$, KtyI$^{-/-}$ K14wt and KtyI$^{-/-}$ K14.R131P) were established and cultured as described previously (Homberg *et al.*, 2015; Kröger *et al.*, 2013; Kumar *et al.*, 2015; Ramms *et al.*, 2013).

Immunofluorescence analysis and image processing

Keratinocytes grown on coverslips were fixed for 3min in methanol (-20°C). Primary antibodies were diluted in 1% (w/v) BSA in Tris-Buffered Saline (TBS) and incubated overnight at 4°C in a humid chamber (Table S1). The next day, coverslips were washed in TBS and incubated with the fluorophore-conjugated secondary antibody and HCS CellMask^{TM} Stain (CMR, Invitrogen) for 30min at RT in the dark. DNA was stained with DAPI. Finally, coverslips were washed three times in TBS, rinsed briefly in aqua bidest? and mounted with ProLong® Gold antifade reagent (Invitrogen).

For immunofluorescence after extraction of soluble proteins, coverslips were washed with PBS and then with cytoskeleton stabilizing buffer (CSB; 4 M glycerol, 25 mM PIPES, 1 mM EGTA, 1 mM MgCl$_2$), incubated in CSB + 0.2% Triton X-100 for 5min. Fixation was performed in 4% formalin for 30min at room temperature. After fixation, coverslips were washed in PBS, CSB washing buffer 1 (0.02% Tween-20/PBS) and CSB washing buffer 2 (1% BSA/0.02% Tween-20/PBS) for 5 min each. Primary (Table S1) and secondary

antibodies were diluted in CSB blocking solution and incubated for 1h or 30 min, respectively, washing with TBS between incubation steps. Finally, coverslips were washed with CSB washing buffer 1 for 5 min, dried and mounted as described above.

Images were acquired in sequential scan mode with a Zeiss LSM 780 confocal microscope equipped with 63x/1.4 Plan-Apochromat Oil DIC M27 objective and Airyscan-Module under standard settings (illumination at 488nm and 561nm). The size of the pinhole was always set to 1 Airy unit. Image analysis was performed using Zen Black Software 2.3 (Carl Zeiss, Inc.). ImageJ was used for image processing and line scan analysis of K14 and CMR fluorescence intensities across keratin aggregates. Figures were designed with Scribus 1.5.8. Software.

Cytoskeletal preparation

To separate soluble from insoluble proteins, 6×10^5 keratinocytes were seeded on a 60 mm dish. Cells were washed with PBS, scraped off with a cell scraper in ice-cold low-salt buffer (10 mM Tris-HCl pH 7.6, 140 mM NaCl, 5 mM EDTA, 5 mM EGTA, 0.5% Triton X-100) supplemented with 1x Halt protease Inhibitor, 1x Phosphatase Inhibitor, RNase (5 μg/ml) and DNase (2.5 μg/ml). Lysate was homogenized with a douncer and centrifuged for 10 min at 5,000 x g (4°C). Supernatant was collected and precipitated with 5% trichloroacetic acid. Pellet was homogenized with a douncer in ice-cold high-salt buffer (10 mM Tris-HCl pH 7.6, 140 mM NaCl, 1.5 M KCl, 5 mM EDTA, 5 mM EGTA, 1% Triton X-100) supplemented with 1x Halt protease Inhibitor, 1x Phosphatase Inhibitor, RNase (5 μg/ml) and DNase (2.5 μg/ml). Following incubation on ice for 30 min, the homogenate was centrifuged for 10 min at 15,000 x g (4°C). The supernatant was discarded and the pellet was resuspended in the same buffer. This procedure was repeated 3 times. After centrifugation for 10 min at 15,000 x g (4°C) the resulting pellet, representing the insoluble keratin-enriched fraction, was resuspended in Laemmli lysis buffer with repeated cycles of heating (98°C) and sonication. Samples were stored at -80°C. For further proteomic analysis of keratin-enriched pools, the pellet was washed with sterile water and vortexed briefly. Then, samples were centrifuged for

2 min at 10,000 x g and the supernatant was discarded. This step was repeated; then samples were dried in a SpeedVac (Uniequip) and stored at -80°C until further processing.

Proteomics

Cytoskeletal (insoluble) fractions of KtyI$^{-/-}$ K14wt and K14.R131P keratinocytes were prepared as described above and processed as described in (Kumar *et al.*, 2015): samples were dissolved in 2% sodium dodecanoate, 50 mM ammonium bicarbonate, 25 mM dithiothreitol and then alkylated with 50 mM iodoacetamide at RT in the dark with stirring. The digest was acidified with TFA, extracted three times with ethyl acetate, brought to pH 8 with ammonia and ammonium bicarbonate buffer, digested with reductively methylated bovine trypsin and analyzed using a Q-Exactive mass spectrometer (Thermo Scientific). Searching of the Uniprot_database (20140310; 87,012 entries) was performed with X! Tandem (version CYCLONE (2013.02.01.1; GPM), and Scaffold software (version 4.4.1.1; Avontus Software) was used to validate MS/MS based peptide and protein identifications as previously described (Laatsch *et al.*, 2014; Rice *et al.*, 2013). False discovery rates were estimated as 0.2% for peptide and 2.6% for protein identifications based on a decoy peptide library. Results are shown in Supplementary Table 2 illustrated by weighted (after verification of the protein presence by exclusive spectral counts in protein clusters with shared peptides) and exclusive spectral counts. Both types of count arrive at the same significant changes comparing K14 R131P to K14 WT. The significant changes of the exclusive spectral counts from K14 R131P in comparison to K14 WT are shown in Figure 2d. Sample preparation and mass spectrometry analysis were performed by the Proteomics Core, UC Davis, California, USA essentially as previously described [9, 10].

SDS-PAGE and immunoblot analysis

To separate proteins under denaturing conditions, sodium dodecyl sulfate polyacrylamide gel electrophoresis (SDS-PAGE) was performed. Gels were then either processed for immunoblot

analysis or stained with Coomassie Brilliant Blue. For immunoblot analysis, proteins were transferred to nitrocellulose membranes (VWR) using a semi-dry blotter (Armin Baack Labortechnik). Membranes were blocked using 3% (w/v) skim milk/TBS with Tween (TBST) and subsequently probed with K14 antibody (Table S1). Chemiluminescence was detected using ChemoCam Imager (Intas).
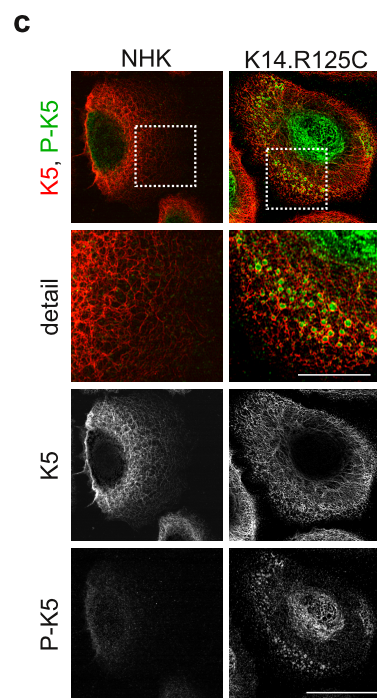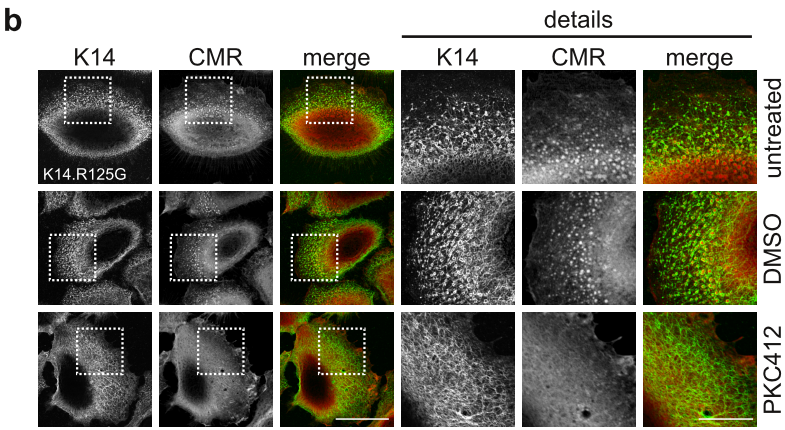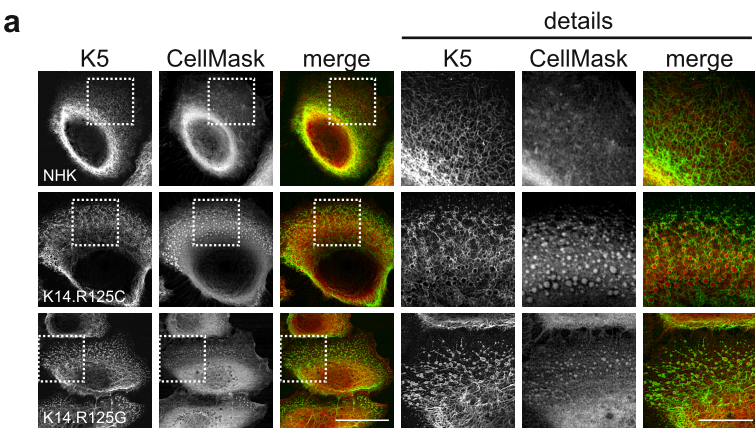
<u>Statistics</u>

All statistics were processed using GraphPad Prism software, version 9.

SUPPLEMENTARY FIGURE LEGENDS

Figure S1. CMR dye stains EBS-associated K14.R125C and K14.R125G keratin aggregates.

(a) Immortalized patient-derived K14.R125C, K14.R125G and normal human keratinocytes (NHK) were analyzed by immunofluorescence microscopy showing K5 and CellMask Red (CMR) dye. Depicted are confocal images of single optical sections. The enlargements highlight the labeling of keratin aggregates by CMR. Scale bar: 25µm, details: 10µm. **(b)** EBS K14.R125G keratinocytes were treated with PKC412 or DMSO for 24h, respectively, and immunostained for K14 and CMR. Depicted are confocal images of single optical sections. Scale bar: 25µm, details: 10µm. **(c)** K14.R125C and NHK were analyzed by immunofluorescence microscopy showing phosphorylated K5 at T150 (P-K5 in green) and K5 (in red). Depicted are confocal images of single optical sections. Scale bar: 25µm, details: 10µm.

a

	K5	CellMask	merge	details		
				K5	CellMask	merge

NHK

K14.R125C

K14.R125G

b

	K14	CMR	merge	details		
				K14	CMR	merge

K14.R125G

untreated

DMSO

PKC412

c

NHK   K14.R125C

K5, P-K5

detail

K5

P-K5

SUPPLEMENTARY TABLES

Table S1. List of antibodies including dilutions used in immunoblot (IB) analysis and immunofluorescence (IF) staining.

Primary antibody	Source	Host	IB dilution	IF dilution
K5	Magin lab	rabbit		1:100
Phospho-K5 (T150) = Phospho-K8 (S73) [LJ4]	Merck	mouse		1:500
K14	Magin lab	rabbit	1:25,000	1:100
K14 [LL002]	Abcam (ab7800)	mouse		1:100
Secondary antibody	**Source**	**Host**	**IB dilution**	**IF dilution**
anti-mouse-A488	Dianova	Donkey		1:800
anti-rabbit-A488				
anti-rabbit-Cy3				
anti-rabbit HRP			1:20,000	

SUPPLEMENTARY REFERENCES

[1] Has C, Kusel J, Reimer A, Hoffmann J, Schauer F, Zimmer A*, et al.* (2018) The Position of Targeted Next-generation Sequencing in Epidermolysis Bullosa Diagnosis. *Acta Dermato-Venereologica* 98:437-40.

[2] He Y, Maier K, Leppert J, Hausser I, Schwieger-Briel A, Weibel L*, et al.* (2016) Monoallelic Mutations in the Translation Initiation Codon of KLHL24 Cause Skin Fragility. *American Journal of Human Genetics* 99:1395-404.

[3] Homberg M, Ramms L, Schwarz N, Dreissen G, Leube RE, Merkel R*, et al.* (2015) Distinct Impact of Two Keratin Mutations Causing Epidermolysis Bullosa Simplex on Keratinocyte Adhesion and Stiffness. *The Journal of Investigative Dermatology* 135:2437-45.

[4] Kumar V, Bouameur JE, Bar J, Rice RH, Hornig-Do HT, Roop DR*, et al.* (2015) A keratin scaffold regulates epidermal barrier formation, mitochondrial lipid composition, and activity. *The Journal of Cell Biology* 211:1057-75.

[5] Kröger C, Loschke F, Schwarz N, Windoffer R, Leube RE, Magin TM (2013) Keratins control intercellular adhesion involving PKC-alpha-mediated desmoplakin phosphorylation. *The Journal of Cell Biology* 201:681-92.

[6] Ramms L, Fabris G, Windoffer R, Schwarz N, Springer R, Zhou C*, et al.* (2013) Keratins as the main component for the mechanical integrity of keratinocytes. *Proceedings of the National Academy of Sciences of the United States of America* 110:18513-8.

[7] Rice RH, Bradshaw KM, Durbin-Johnson BP, Rocke DM, Eigenheer RA, Phinney BS*, et al.* (2012) Differentiating inbred mouse strains from each other and those with single gene mutations using hair proteomics. *PloS One* 7:e51956.

[8] Laatsch CN, Durbin-Johnson BP, Rocke DM, Mukwana S, Newland AB, Flagler MJ*, et al.* (2014) Human hair shaft proteomic profiling: individual differences, site specificity and cuticle analysis. *PeerJ* 2:e506.

[9] Rice RH, Durbin-Johnson BP, Salemi M, Schwartz ME, Rocke DM, Phinney BS (2017) Proteomic profiling of Pachyonychia congenita plantar callus. J Proteomics 165: 132–137

[10] N. Karim, B. Durbin-Johnson, D.M. Rocke, M. Salemi, B.S. Phinney, M. Naeem, et al., Proteomic manifestations of genetic defects in autosomal recessive congenital ichthyosis, J Proteomics 201 (2019) 104-109.